

Bigfoot Spectral Cell Sorter with Sasquatch Software

The world's first real-time spectral cell sorter

Introduction

Researchers working in flow cytometry require the highest-quality data from every sample in order to achieve increasingly challenging scientific goals. The demand for higher-resolution, multidimensional data has amplified interest in spectral data unmixing and analysis as compared to the traditional method of compensation for spectral spillover. Investigators frequently find it difficult or impossible to resolve dim, rare, or highly autofluorescent populations using standard compensation. Although some companies offer spectral analysis and post-acquisition sort solutions, workflows are cumbersome, and experiments consume large volumes of precious sample. Despite the shortcomings of current options, researchers still desire the power of spectral data handling. The Invitrogen™ Bigfoot Spectral Cell Sorter was developed with innovative hardware and software specifically to sort cells using spectrally unmixed data in real time.

Seventeen years ago, the concept of spectral flow cytometry was demonstrated by flow cytometry pioneer and innovator J. Paul Robinson, Cytometry Lab, Purdue University, but it was not incorporated into standard instruments for many years due to limited practical applications [1]. In 2015, commercial spectral flow cytometers appeared on the market ready for installation in core lab facilities seeking to take on new challenges (Futamura 2015) [2]. These instruments still offer a chance to unravel complex, heterogeneous populations where autofluorescence limits dye options (Schmutz 2017) [3]. This type of versatility is reshaping panel design by allowing freedom to combine fluorescent proteins, surface markers, and other dyes while still allowing spectral separation.



However, many instruments that are produced today are uniquely configured to primarily perform spectral analysis, with limited options to perform the accepted, reliable, and trusted technique of compensation, which some researchers still want due to familiarity or for comparison to other methods. The Bigfoot Spectral Cell Sorter's acquisition and sorting application, Sasquatch Software (SQS), allows the operator to sort and analyze either spectrally unmixed data or traditional compensated data.

As with most technological tools, the quality of data produced depends on proper use. Successful high-speed sorting on spectrally unmixed data requires a precise combination of concepts from the disciplines of biology, mathematics, and high-speed computing. Some researchers may find it overwhelming to balance numerous fields of expertise, where even a slight knowledge gap can result in suboptimal experiment design and results. We used the underlying mathematical theory of spectral data handling to develop tools that provide researchers with valuable guidance, starting with panel design and continuing throughout all phases of the experiment. Not only does this impart mathematical rigor and eliminate subjectivity, it also frees the researcher to focus on his or her scientific specialty. SQS includes extensive user-support tools to identify fluorophores that, when paired, are either expected to unmix properly or are expected to be challenging due to high levels of signal overlap. To assist with experiment design, geometric and statistical comparisons are performed to assess the likelihood of successful unmixing of the chosen panel. Similar comparisons are used to identify and account for autofluorescence. The spectral unmixing process is performed on specialized, state-of-the-art hardware, allowing for remarkably fast real-time processing and high-purity spectral sorting.

In this paper, we will demonstrate the capability of the Bigfoot Spectral Cell Sorter using a fifteen-color panel (Figure 1). This panel was selected to show proof of principle for this cutting-edge technique of combining spectral workflow and multiparameter six-way cell sorting. Hardware features are covered in more detail in the “Discussion and conclusion” section of this white paper, as well as in other white papers [4, 5].

Methods

The Bigfoot Spectral Cell Sorter was started and allowed to warm up and stabilize for 10 minutes, after which the automated QC process was initiated. The comprehensive three-bead QC protocol set the optimal nozzle position, calibrated droplet and stream settings, adjusted the stream positions, and calculated the system’s drop delay value. The resulting CVs, voltages, and separation factor, as well as sort settings, are tracked day-to-day and can be viewed in a trending report. PMT voltages can be applied as application references in future experiments.

Sample preparation

Normal human peripheral blood mononuclear cells (PBMCs) were collected from donors and immediately stained with the fluorophore-conjugated antibodies, including single color controls, at optimal concentrations for unstained-stained signal separation. The blood was then lysed using OptiLyse™ C solution (Beckman Coulter; Cat. No. A11895) for 10 minutes. After lysing, a buffer solution of Hanks’ balanced salt solution (HBSS) and 2% fetal bovine serum (FBS) was added to increase the quality and longevity of the sample. The samples were then centrifuged at 300 x g for 5 minutes and the supernatant was removed. HBSS was added to each sample and immediately run on the Bigfoot Spectral Cell Sorter using SQS. The sample used for sorting was further concentrated to allow for a higher event rate and sort speed.

Laser	Antigen	Color	Vendor	Cat. No.	Clone
349	CD4	BUV395	BD Horizon	563550	SK3
405	CD127	BV421	BioLegend	351310	A019D5
405	CD16	BV510	BioLegend	302048	3G8
405	CD45RA	BV711	BioLegend	304137	HI100
405	CD45RO	BV786	BioLegend	304233	UCHL1
405	CD27	Pacific Blue	BioLegend	302822	0323
488	CD45	FITC	Invitrogen	11-0459-42	HI30
488	CD3	Alexa 532	Invitrogen	58-0038-42	UCHT1
488	TCRgd	PerCP-eFluor 710	Invitrogen	46-9959-42	B1.1
561	CD56	PE	BioLegend	318306	HCD56
561	CD19	PE-Cy5.5	Invitrogen	35-0198-42	SJ25C1
561	CD14	PE-Cy7	Invitrogen	25-0149-41	61D3
561	CD25	PE-eFluor 610	Invitrogen	61-0257-42	CD25-4E3
640	CD20	Alexa 700	Invitrogen	56-0209-42	2H7
640	CD8	APC	BioLegend	344722	SK1

Figure 1. 15-color fluorophore panel.

Spectral workflow

In SQS, a new sort workflow was selected and designated as a spectral experiment. The required fluorophores were selected (Figures 2–4) and single-color control samples and templates were automatically generated. The unstained control was placed on the multisample loader and run on the instrument. PMT voltages were automatically set to ensure that autofluorescence signals were resolved. Without any additional voltage adjustments, the single-color controls were run sequentially using the multisample loader and the automatically generated templates were populated with data. The instrument obtained the spectral signature for each fluorophore in all fluorescence channels. The unmixing algorithm automatically applied calculations after each control was acquired and recorded. New “unmixed parameters” then became selectable in plots and were used for acquisition and sorting in the workspace. Spectral plots were automatically created in all fluorescence channels; a few examples are shown in Figures 5–9.

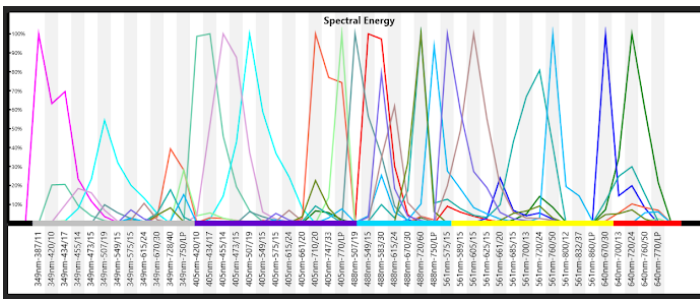


Figure 2. SQS presents a visual representation of the selected panel of fluorophores. This graph is helpful as it provides a clear picture of where additional fluorophores can be added without overlapping with the current selections. A specific emission curve can be shaded by highlighting it in the “Selected fluorophores” list.

	CD3 Alexa 532	CD20 Alexa 700	CD8 APC	CD4 BUV 395	CD127 BV 421	CD16 BV 510	CD45RA BV 711	CD45RO BV 786	CD45 FITC	CD27 Pacific Blue	CD19 PE-Cy5.5	CD14 PE-Cy7	CD25 PE-eFluor	TCRgd PerCP-eF	CD56 PE
CD3 Alexa 532	0.00	0.00	0.00	0.00	0.02	0.00	0.00	0.52	0.00	0.06	0.16	0.30	0.02	0.48	
CD20 Alexa 700	0.00	0.29	0.00	0.00	0.00	0.16	0.03	0.00	0.00	0.35	0.09	0.01	0.13	0.00	
CD8 APC	0.00	0.29	0.00	0.00	0.00	0.03	0.00	0.00	0.00	0.21	0.02	0.05	0.06	0.02	
CD4 BUV 395	0.00	0.00	0.00	0.14	0.04	0.00	0.01	0.00	0.07	0.00	0.00	0.00	0.00	0.00	
CD127 BV 421	0.00	0.00	0.00	0.14	0.12	0.02	0.07	0.00	0.55	0.00	0.00	0.00	0.00	0.00	
CD16 BV 510	0.02	0.00	0.00	0.04	0.12	0.01	0.01	0.15	0.46	0.01	0.01	0.02	0.02	0.02	
CD45RA BV 711	0.00	0.16	0.03	0.00	0.02	0.01	0.57	0.00	0.03	0.13	0.08	0.00	0.18	0.00	
CD45RO BV 786	0.00	0.03	0.00	0.01	0.07	0.01	0.57	0.00	0.05	0.01	0.09	0.00	0.02	0.00	
CD45 FITC	0.52	0.00	0.00	0.00	0.15	0.00	0.00	0.02	0.02	0.07	0.10	0.01	0.17	0.00	
CD27 Pacific Blue	0.00	0.00	0.00	0.07	0.55	0.46	0.03	0.05	0.02	0.00	0.00	0.00	0.00	0.00	
CD19 PE-Cy5.5	0.06	0.35	0.21	0.00	0.00	0.01	0.13	0.01	0.02	0.00	0.31	0.13	0.55	0.14	
CD14 PE-Cy7	0.16	0.09	0.02	0.00	0.00	0.01	0.08	0.09	0.07	0.00	0.31	0.19	0.14	0.30	
CD25 PE-eFluor 610	0.30	0.01	0.05	0.00	0.00	0.02	0.00	0.00	0.10	0.00	0.13	0.19	0.05	0.59	
TCRgd PerCP-eFluor 710	0.02	0.13	0.06	0.00	0.00	0.02	0.18	0.02	0.01	0.00	0.55	0.14	0.05	0.02	
CD56 PE	0.48	0.00	0.02	0.00	0.00	0.02	0.00	0.00	0.17	0.00	0.14	0.30	0.59	0.02	

Figure 3. The spectral similarity matrix of SQS allows the user to identify fluorophore combinations that cause an increase in complexity and may be more difficult to spectrally unmix.

■ Alexa 532	CD3	Alexa 532	1.00 ×
■ Alexa 700	CD20	Alexa 700	1.00 ×
■ APC	CD8	APC	1.34 ×
■ BUV 395	CD4	BUV 395	1.34 ×
■ BV 421	CD127	BV 421	1.34 ×
■ BV 510	CD16	BV 510	1.34 ×
■ BV 711	CD45RA	BV 711	1.40 ×
■ BV 786	CD45RO	BV 786	2.00 ×
■ FITC	CD45	FITC	2.00 ×
■ Pacific Blue	CD27	Pacific Blue	2.37 ×
■ PE-Cy5.5	CD19	PE-Cy5.5	2.38 ×
■ PE-Cy7	CD14	PE-Cy7	2.41 ×
■ PE-eFluor 610	CD25	PE-eFluor 610	2.45 ×
■ PerCP-eFluor 710	TCRgd	PerCP-eFluor 710	2.56 ×
■ PE	CD56	PE	2.78 ×

Figure 4. As the investigator selects fluorophores, the complexity index on the right of this panel tracks the quality of the overall panel. The value increases when there is more predicted overlap between spectral signatures. Fluorophores that minimally increase the index value are ideal choices.

Spectral plot examples

The autofluorescence background signal is captured using the unstained control. SQS uses an automated positive signal selection process, which often means that only a small number of positive events are required to construct the single-color-control signal. For each signal, the process automatically seeks significant separation from the autofluorescence of the unstained sample, thus ensuring a robust positive single-color-control signal. With this information, the software defines the positive populations, which are then shown in automatically generated templates. Successful experiments have been run with as few as 50 positive events, showing that SQS can build quality spectral signals remarkably fast. These efficiencies mean less sample waste and reduced setup time.

A spectral graph is included in each of the automatically generated single control templates showing the signature of the positive cells in each control. Some examples of these are shown in Figures 5–9. The variation in spectral curves between different fluorophores is key to the unmixing algorithms applied to the data.

Cell sorting setup

Six populations were selected for sorting, highlighting the ability to combine spectral unmixing and cell sorting. These populations are identified by the outlined gating strategy (Figures 10–21). The Bigfoot Spectral Cell Sorter was configured with a 100 μm nozzle tip, 30 psi sheath pressure, a drop drive amplitude of 13.3 volts, and a drop drive frequency of 40,600 Hz. The sort was performed with an event rate of 5,000 events per second on the identified spectrally unmixed populations. Cells were sorted using purity mode into six 5 mL tubes with 500 μL filtered HBSS and reanalyzed for purity.

Gating strategy

Normal human PBMC

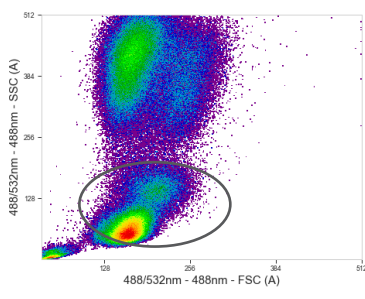


Figure 10. FSC vs. SSC plot with a gate drawn to include lymphocytes and monocytes.

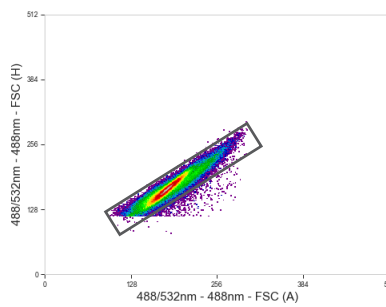


Figure 11. FSC area vs. height plot gated on the gate from the FSC vs. SSC plot. The singlets region is drawn to include single cells and exclude doublets.

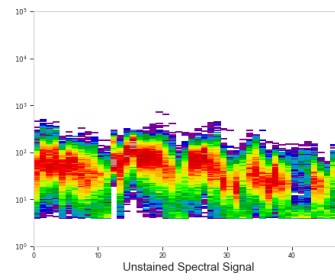


Figure 5. Spectral signal from the unstained sample.

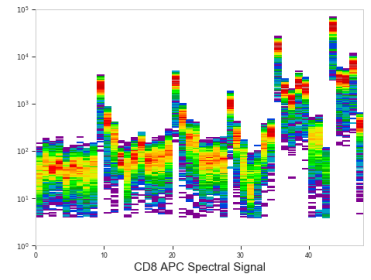


Figure 6. Spectral signal from single-stained CD8 APC sample.

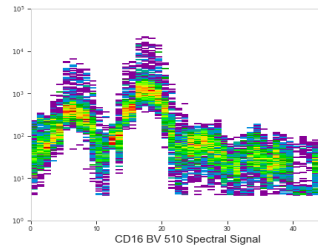


Figure 7. Spectral signal from single-stained CD16 BV 510 sample.

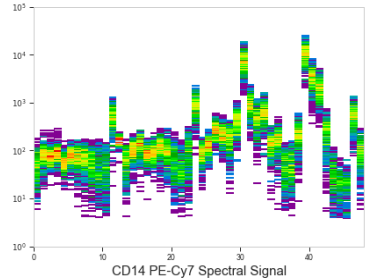


Figure 8. Spectral signal from single-stained CD14 PE-Cy7[®] sample.

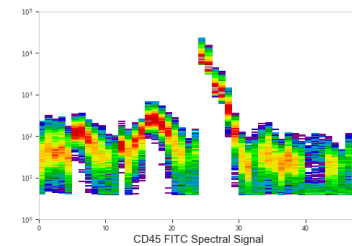


Figure 9. Spectral signal from single-stained CD45 FITC sample.

Monocytes and B cells resolved

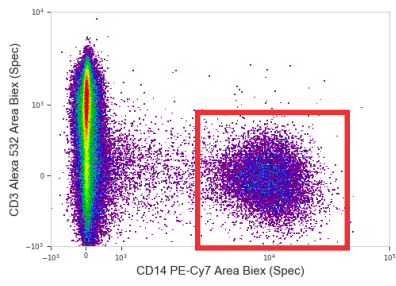


Figure 12. The CD14 vs. CD3 plot is gated on scatter and singlets. The sort gate is drawn to sort CD14 positive monocytes.

Lymphocyte gating

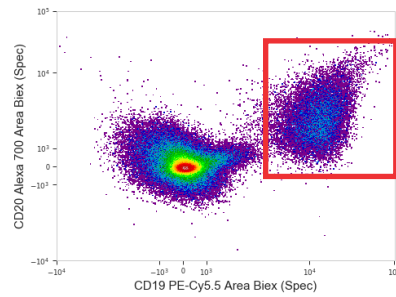


Figure 13. The CD19 vs. CD20 plot is gated on scatter and singlets. The sort gate is drawn to sort CD19 and CD20 positive B cells.

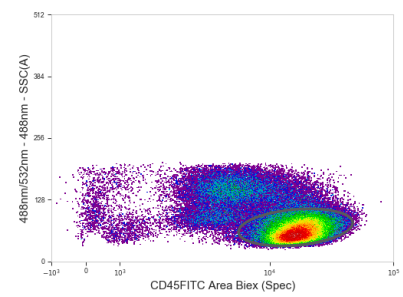


Figure 14. The CD45 vs. SSC plot is gated on scatter and singlets to identify CD45 positive subsets. The gate is drawn on the CD45 high, side scatter low, population to identify lymphocytes.

NK cell subpopulation identification

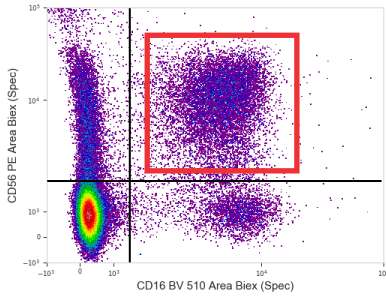


Figure 15. The CD16 vs. CD56 plot is gated on scatter, singlets, and lymphocytes. The sort gate is drawn to identify dual positive cells. The sort priority was set lower than the CD8 CD56 dual positive population.

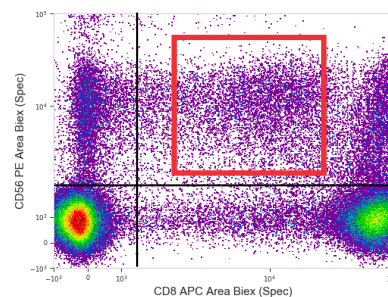


Figure 16. The CD8 vs. CD56 plot is gated on scatter, singlets, and lymphocytes. The sort gate is drawn to identify CD56 positive CD8 dim cells (cytotoxic T cells). The sort priority was set higher than the CD16 CD56 dual positive population.

CD3 positive T cell subsets

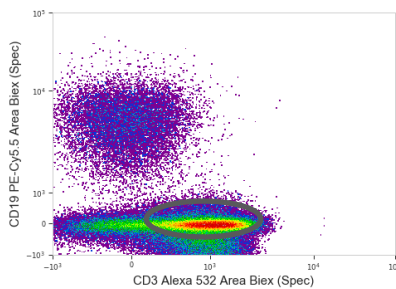


Figure 17. The CD3 vs. CD19 plot is gated on scatter, singlets, and lymphocytes. The gate is drawn to identify CD3 positive cells.

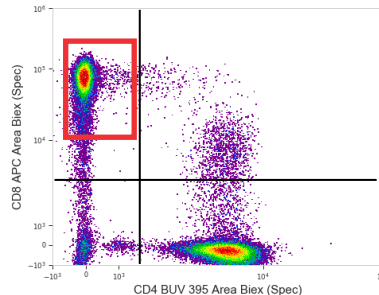


Figure 18. The CD4 vs. CD8 plot is gated on scatter, singlets, lymphocytes, and CD3 positive cells. The sort gate is drawn to identify CD8 strong-positive cells. The quadrant is drawn and Q4 is used to gate CD4 positive cells.

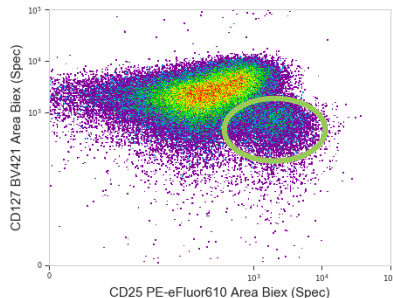


Figure 19. The CD25 vs. CD127 plot is gated on scatter, singlets, lymphocytes, CD3 positive cells, and CD4 positive cells. The sort gate is created to sort Treg cells.

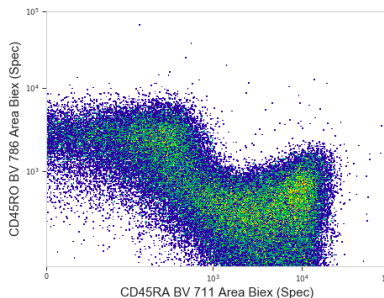


Figure 20. Gated CD4 positive T cells displaying CD45ra and CD45ro expression profiles.

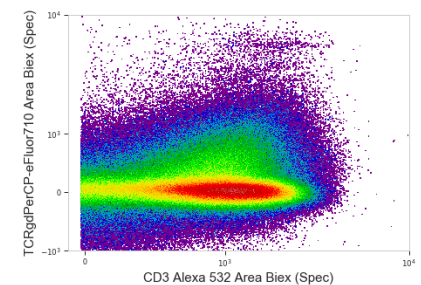


Figure 21. The CD3 vs. TCRgd plot is gated on scatter, singlets, lymphocytes, and CD3 positive cells identifying the TCRgd population.

Results

Following the sort, each collection tube was reanalyzed for purity and examples of the results are shown in Figures 22–25. The spectral unmixing capability of the Bigfoot Spectral Cell Sorter produced results with high efficiency and greater than 98 percent purity. The sorting performance is equivalent to instruments that utilize traditional compensation. This parity will allow users to seamlessly transition between the two methods as experiment complexity increases, thus improving research laboratory workflow.

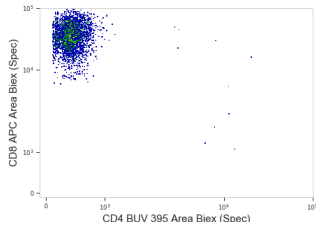


Figure 22. CD8 strong positive population.

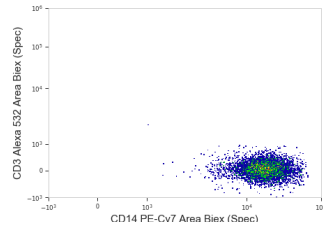


Figure 23. CD14 positive monocytes.

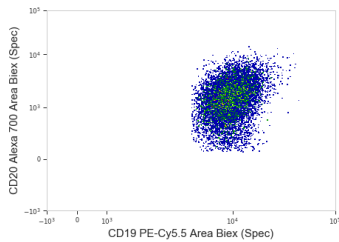


Figure 24. CD19, CD20 positive B cells.

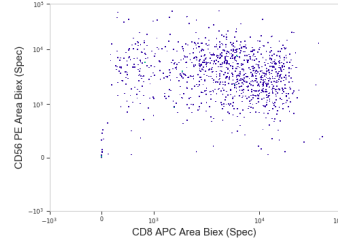


Figure 25. CD8 dim, CD56 positive cytotoxic T cells.

Discussion and conclusion

Full spectral cytometry has been proven to help researchers build complex panels with numerous and novel combinations of markers. The data retrieved from these experiments are well resolved and of higher resolution than is possible with traditional methods. However, the Bigfoot Spectral Cell Sorter takes these improvements to the next level by enabling these new combinations of markers to be sorted in real time. Additionally, operators can select up to 18 subpopulations of cells and sort each one to a different tube in a single run, or utilize the reverse index feature to correlate an event in a plot with the physical location of the sorted event in a plate to further support DNA sequencing.

The ability to compare two fluorochromes across multiple points on their spectra significantly reduces the correction error compared to compensating two spectral bands. Full spectrum sorting will produce better population resolution compared to nonspectral sorting, and so result in superior sorted populations.

The electronics of the Bigfoot Spectral Cell Sorter include custom-designed, programmable-logic hardware with algorithms developed specifically for the challenges presented by sorting. Multiple innovations and design iterations were required to achieve greater than six terabits per second data processing speed required for successful operation. The resulting architecture allows operators to use either compensation or spectral unmixing in real time at a sort rate of >70,000 events per second.

The Bigfoot Spectral Cell Sorter has up to nine lasers with 3–12 PMTs available for each detection path, and is therefore ideally suited for the wide range of fluorescence signal intensities found in diverse flow cytometry applications. PMT voltages can be set using a control sample of unstained cells or by importing application settings derived from a three-bead QC control. The Bigfoot Spectral Cell Sorter was designed using PMTs because they provide robust signal strength, which results in a higher signal-to-noise ratio than other collection methods. Furthermore, PMTs paired with selected single-channel filters (Figure 26) create improved differentiation of fluorophore spectra and ensure that the system is not limited to a specific application. The Bigfoot Spectral Cell Sorter's PMTs have an 8 mm diameter aperture, which significantly improves signal stability, resulting in narrow CVs and consistent results across flow rates for the entire workday. The detector and optical configuration designed into the Bigfoot Spectral Cell Sorter allow investigators the option of viewing data in multidimensional spectral mode or with compensation; both methods achieve outstanding performance. No other instrument can provide these advantages to the researcher.

invitrogen

The power of spectral flow cytometry and real-time sorting can help to extend the frontier of cell-type discovery in the immediate future. The combination of expanded panel options with high-throughput cell sorting enables the rapid interrogation of novel populations. Thus, the Bigfoot Spectral Cell Sorter offers particular promise for large-scale exploratory efforts such as the Human Cell Atlas, where spectral sorting will likely expand the ability to identify and isolate new cell populations (Regev 2017) [6]. Further, these novel multiparametric panels are expected to provide expanded protein expression information to complement transcriptional characterization of novel human cell types by high-throughput sequencing.



Figure 26. PMTs and filters on the Bigfoot Spectral Cell Sorter.

As part of our continuing efforts to be responsive to professionals working in flow cytometry, our team engages in ongoing dialog with industry experts to deliver the features and performance needed for high-end instrumentation. The Bigfoot Spectral Cell Sorter is the product of decades of flow cytometry experience, innovative engineering, and constant collaboration. As the first spectral cell sorter, the Bigfoot Spectral Cell Sorter will expand research capabilities and provide innovation to serve those in the quest for greater scientific knowledge.

References

1. Robinson, J. Paul, Cytometry Lab, Purdue University, Spectral flow cytometry—*Quo vadimus?* <https://onlinelibrary.wiley.com/doi/full/10.1002/cyto.a.23779>
2. Futamura, K., Sekino, M., Hata, A., Ikebuchi, R., Nakanishi, Y., Egawa, G., Kabashima, K., Watanabe, T., Furuki, M. and Tomura, M. (2015), Novel full-spectral flow cytometry with multiple spectrally-adjacent fluorescent proteins and fluorochromes and visualization of *in vivo* cellular movement. *Cytometry*, 87: 830–842. doi:10.1002/cyto.a.22725
3. Schmutz, S., Valente, M., Cumano, A., Novault, S., Analysis of cell suspensions isolated from solid tissues by spectral flow cytometry. *J. Vis. Exp.* (123), e55578, doi:10.3791/55578 (2017).
4. Helm, K. et al., Bigfoot Spectral Cell Sorter—A new approach to cell sorter safety. 20 May 2020.
5. Kissner, M. et al., Bigfoot Spectral Cell Sorter—High-throughput plate sorting. 20 May 2020.
6. Regev, Aviv, Sarah A Teichmann, Eric S Lander, Ido Amit, Christophe Benoist, Ewan Birney, Bernd Bodenmiller, et al. "The Human Cell Atlas." Edited by Thomas R Gingeras. *ELife* 6 (December 5, 2017): e27041. <https://doi.org/10.7554/eLife.27041>.

Find out more at thermofisher.com/bigfoot

ThermoFisher
SCIENTIFIC